IEEE Access
Multidisciplinary | Rapid Review | Open Access Journal

Received 4 December 2023, accepted 15 December 2023, date of publication 18 December 2023,
date of current version 28 December 2023.

Digital Object Identifier 10.1109/ACCESS.2023.3344452

RESEARCH ARTICLE

Canine Biometric Identification Using ECG Signals and CNN-LSTM Neural Networks

MIN KEUN CHO AND TAE SEON KIM
School of Information, Communications, and Electronics Engineering, The Catholic University of Korea, Bucheon-si, Gyeonggi-do 14662, Republic of Korea
Corresponding author: Tae Seon Kim (tkim@catholic.ac.kr)

This work was supported by The Catholic University of Korea, Research Fund, in 2021.

ABSTRACT As global pet acceptance increases, the market size for pet ownership grows. Consequently, registering pets is becoming increasingly crucial, with some nations mandating it by law. Animal biometrics is a subject of ongoing research, spanning inscriptions, iris recognition, and facial recognition, with a growing number of companies partaking. However, biometric methods mostly rely on image recognition, which can result in degraded performance depending on the captured angle and external environment. To address this issue, we conducted a study to design and evaluate the performance of a deep learning-based dog identity recognition system that utilizes electrocardiogram (ECG) that is harder to forge than existing methods and does not require additional image processing. To evaluate performance, we utilized two dog ECG databases and conducted biometric recognition experiments with data collected from differing measurement environments from these integrated databases. Input signals for recognition were generated through both R-peak based and blind signal segmentation methods. For the purpose of dog identification, we developed and employed a 1D CNN-LSTM model as a classifier. Additionally, three DNN-based classifiers were developed to compare their performance with that of the proposed model. To evaluate performance, the confusion matrix was used in conjunction with metrics such as accuracy, equal error rate (EER), receiver operating characteristic (ROC) curve, and precision recall (PR) curve. The proposed model demonstrated up to 98.7% accuracy in the biometrics of a separate database of 16 subjects, and as high as 96.3% accuracy in the biometrics of an integrated dataset of 33 subjects. The suggested approach exhibited a 93.1% accuracy rate when employing the blind segmentation method, eliminating the need for supplementary signal processing to derive input signals.

INDEX TERMS Biometrics, canine identification, deep learning, electrocardiogram (ECG) signal.

I. INTRODUCTION

The number of households owning pets is increasing rapidly, with corresponding growth in the pet market. This trend is attributed to heightened awareness of animal welfare, as well as the rise in aging and single populations internationally. Furthermore, the COVID-19 pandemic has amplified demand for pets as people have the opportunity to spend more time at home. A survey by Forbes Advisor revealed that 78% of pet owners obtained their furry companions amidst the pandemic [1]. However, the heightened demand for pets has coincided with a surge in pet abandonment, as society navigates its way through the aftermath of the pandemic, leading to a global crisis in abandoned animals. Estimates of the total number of pets worldwide vary depending on the source and definition, but Health for Animals, a global animal health association, estimates that the number of pets in the world exceeds one billion, with over half of the world's population owning a pet at home [2].

In the United States, 86.9 million households have pets in 2023, of which 65.1 million have dogs [1]. Based on the data provided by the Best Friends Animal Society, the rise in

The associate editor coordinating the review of this manuscript and approving it for publication was Zahid Akhtar.

the number of pets admitted to animal shelters in 2022 was primarily influenced by the increase in abandoned dogs, which accounted for 54% of all admissions [3]. Amongst all pets, dogs also have the highest proportion in South Korea. While official 2022 stray animal statistics have not yet been released by the government, a study by the Animal Freedom Alliance revealed that approximately 110,000 animals were brought to animal care facilities in 2022 due to irresponsible or intentional abandonment by their owners [4]. Among these, dogs comprised 71.3% of the total, with around 44.1% of them unable to be reunited with their original owners and subsequently passing away in shelters due to euthanasia or natural causes. Furthermore, approximately KRW 30 billion is spent each year on sheltering lost and abandoned animals, which is a huge financial loss. As a result of this global trend, pet registration systems are being expanded and implemented at the national level to facilitate disease control and prevent stray animals. Furthermore, the demand for pet insurance is increasing globally. However, pet insurance mainly uses identification tags as a method of pet registration, which can be easily removed, damaged or lost, raising reliability issues.

Common methods of animal registration include ear tagging, freeze branding, tattooing, ear tipping, and registration through radio-frequency identification (RFID) devices [5], [6]. Among these methods, RFID registration, primarily used for pets, can be divided into external (non-invasive) and internal (invasive). External RFID devices typically involve electronic or identification tags that are attached to collars to identify animals. Internal RFID is a microchip implanted in an animal's body for identification purposes [7]. The use of external identifiers raises concerns of loss and duplication, and implantation of chips incurs additional costs, side effects and rejection by the animal [8], [7]. As a result, there is a growing interest in permanent recognition methods that minimize adverse effects, and animal biometrics is currently under exploration as a way to meet these needs.

Biometrics has been widely used in various fields where human identification is required. It uses the unique characteristics of an individual organism for recognition, making them difficult to duplicate and share. Common human biometric techniques include iris recognition [9], fingerprint recognition [10], finger vein recognition [10], facial recognition [11] and ECG based recognition [12], [13]. Among them, the technologies currently applied to animal biometrics include muzzle print, iris recognition, retinal vascular recognition and facial recognition, and other technologies include recognition using external features and recognition through movement patterns [5], [7], [14]. Muzzle print is a common biometric trait used to identify animals by extracting features from the pattern of relative elevation of the skin around the nose, similar to a human fingerprint. This method is mainly used for the identification of livestock such as cows and pigs, and there are also biometric studies using muzzle prints of small animals such as dogs [3], [8], and [15]. Biometric identification using specific patterns extracted from iris and retinal vein images is feasible in the case of animal iris and retinal vein recognition, just as it is in humans. To recognize cattle, it is advantageous to use all facial features including muzzle print, iris and retinal vasculature for biometrics due to their grazing behavior [3]. When applying facial recognition technology designed for humans to animal biometrics, it is feasible to extract facial images by identifying the positions of the eyes, nose, ears, and forehead, and derive features from these images for biometric use. However, further research is necessary to account for changes in appearance caused by growth and the environmental conditions present during image acquisition.

Biometric recognition is accomplished by extracting unique biometric traits from the subject. For biometric identification, the biometric traits must fulfil the following conditions to serve as biometric features [16].

(1) Universality: The biometric characteristic used for identification must be present within the entire population.

(2) Uniqueness: The characteristics of the biometric trait must be different from each other within the population.

(3) Collectability: The biometric trait must be easily acquired and quantifiable.

(4) Circumvention: The characteristics of the biometric trait should not be easily manipulated.

(5) Acceptability: The subject of recognition should not be uncomfortable with the biometric system.

(6) Permanence: The biometric trait should have a small variation over time.

The requirements for traits to be used in biometrics are the same for humans and animals. Therefore, animal biometrics must adhere to the aforementioned prerequisites. In this study, ECG signals were utilized among different biometric traits to identify dogs. In the case of ECG based biometrics, individual human features are extracted from the time-varying waveforms formed by small electrical signals generated during the heartbeat and used for identification. The acquisition of ECG signals in real time is relatively easy, and they have a high degree of universality and uniqueness [17]. Furthermore, given the inherent characteristics of biometric information, its forgery or falsification is challenging, ensuring high levels of security. In this study, we constructed a deep learning network for canine biometrics utilizing ECG signals with beneficial characteristics as delineated above. To date, canine ECG research has been restricted to identifying diseases. However, the similarity of the structure and environment of the canine heart to that of humans has made it a valuable preclinical tool for evaluating QT prolongation in response to different drugs. These similarities between human and canine ECG morphology and conduction time suggest that research on human ECGs can be extended to canine ECGs [18], [19].

This study is significant in that it was the first attempt at biometric identification using canine ECG signals. The aim is to demonstrate the application of human ECG based biometrics, which are more secure and difficult to falsify than image-based biometrics, to dogs. Furthermore, given the lack

of standardized ECG measuring environments, we evaluated the recognition performance by integrating databases with different devices. In addition, we aim to develop a time-series based deep learning dog identification model that maintains its accuracy when using blind segmented ECG signals as input, compared to signals that have been pre-processed to extract single heartbeat waves.

II. RELATED WORKS

A. ANIMAL BIOMETRICS

According to Kühl and Burghardt, animal biometrics is defined as an emerging field for the quantitative representation of species, individuals, behavioral and morphological characteristics [20]. In other words, the field of animal biometrics covers a wider range of studies than the identification of individual object. Research on dog breed classification is mainly based on image information of dogs. Valarmathi et al., for example, developed a method to identify dog breeds from images using computer vision and deep learning algorithms [21]. Their hybrid (Inception-v3 + Xception) model achieved a training accuracy of 98.4% and a validation accuracy of 92.4%. They were able to distinguish targets with high variability both between and within the 120 different breeds with high accuracy based on images of dogs. However, compared to a 1D signal (such as an ECG signal), the model architecture is more complex and the time and hardware resource constraints are inevitably more severe when training the deep learning model with images. As a solution, Wimukthi et al. suggest a more comprehensive approach towards promoting dog well-being. They used various machine learning algorithms to identify the breed and age of dogs from their images, and generated personalized meal plans based on this information, as well as the dog's health and emotional state. They also developed techniques for monitoring dog health and detecting diseases through analysis of barking sounds. The data were taken from the Stanford Dogs Dataset [22] with some non-domestic breeds were removed and twenty mixed-breed dog classes were added. Lai et al. constructed a two-stage based CNN model for dog identification, where the first stage is to classify the dog breed [23]. They employed the Stanford Dogs and Columbia Dogs datasets [22] for dog breed classification and the Flicker-dog dataset [24] for dog identification. Consequently, they improved the identification rate of dogs of the Pug and Husky breeds to 89.94%. Wang et al. devised a technique to solve the dog nose print authentication task of the CVPR 2022 Pet Biometric Challenge [25]. The objective of the challenge was to explore the possibilities of implementing vision-based pattern recognition technology, commonly used for human identification, in the realm of individual dog identification. In other words, the challenge was to capture 20,000 nose print images of 6,000 dogs with a consumer smartphone, use them as training data, and use 2,000 individual images as validation and test data to see the feasibility of nose-print based biometrics for individual dogs. An offline data augmentation technique was implemented to compensate for insufficient training data for each class, resulting in an Area under the ROC curve (AUC) of 86.67%. Li and colleagues participated in the same challenge, presenting a dual global descriptor model that employed a contrastive learning method. They achieved an AUC of 88.8% and won the second place in this challenge [23]. They obtained a recognition accuracy of 98.972% with the Rank-1 approach using a CNN-based deep neural network consisting of a feature extraction module and self-attention modules [8].

As demonstrated in the aforementioned example, conventional biometric dog identification methods mainly use the dog's face or muzzle images as a general approach, and the ECG signal-based dog identification method used in the human authentication method has not yet been announced.

B. ECG AND ECG BASED BIOMETRICS

The ECG is a graph of the electrical changes in the heart that occur during the contraction and relaxation of the heart muscle during a heartbeat. The electrical changes in the heart are due to the potential difference caused by the depolarization and repolarization of cardiac cells [26]. A typical method of acquiring ECG signals is to use conductive paste or gel to measure signals by placing electrodes on the body such as the chest or limbs. However, to facilitate the acquisition of ECG signals and expand applications, off-the-person methods have also been studied, in which sensors are integrated into everyday objects and measured through contact with some body surfaces such as fingertips or palms [26], [27], [28].

ECG has been used to analyze heart diseases including atrial fibrillation and cardiomyopathy for biomedical diagnosis purposes [29], [30], but recently, with the advancement of computing resources and data analysis techniques, biometric recognition using ECG signals has been actively researched [13], [31], [32]. There are two types of feature extraction methods for implementing a human ECG biometric authentication system: ''fiducial feature extraction method'' and ''non-fiducial feature extraction method''. The fiducial method extracts features based on the morphological features of the ECG signal. Put simply, the system detects the ECG fiducial points (P, Q, R, S, T, U) or waveforms such as QRS complexes, and uses the amplitudes, angles and slopes of the signals as individual features [29], [33], [34], [35].

For ECG-based biometrics, the detection of start and end points of a single heartbeat in a continuous ECG signal are required to extract features to be used as inputs to the classifier. In particular, the fiducial feature extraction method extracts features based on the morphological features of the fiducial point, so the decision of the segmentation method and input signal length are important [33]. Petmezas et al. used the R-peak of ECG signals to diagnose atrial fibrillation (AFib) and performed 4-level DWT to detect the R-peak. Then, the segmentation was performed by setting a window of 250 ms ahead and 500 ms behind the R-peak [29]. Luz et al. implemented a window of 800 ms around the R-peak for biometric analysis [36]. AlDuwaile et al. showed

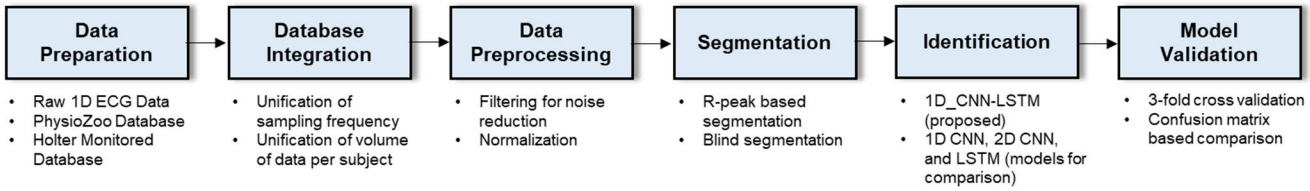

FIGURE 1. Block diagram of proposed canine biometric system.

that shorter signals with a length of 0.5 s around the R-peak for ECG-based biometrics are more efficient for less complex CNN models [13]. Zhang et al. applied blind segmentation of ECG signals with a duration of 2 seconds to biometrics without the use of heartbeat location information [37]. This method requires a wavelet transform to remove the phase difference between randomly selected signals. But it has the advantage of not requiring the effort of extracting fiducial points and improving the generalization performance of the recognition model.

Although no research results on animal biometrics using ECG signals were found, there have been studies on ECG-based biometrics in humans since the mid-2000s, with the latest research mostly based on deep learning neural networks (DNNs) [38]. Furthermore, the early human ECG-based biometric methods mainly used fiducial feature extraction methods, but the trend is changing towards using non-fiducial feature extraction methods or handling the feature extraction process within DNNs themselves [12], [17]. Paiva et al. identified the relative positions of Q, R, S and T fiducial points in ECG signals and extracted the time distance between them as features, which were then applied to authentication using an SVM classifier [39]. The authors showcased the potential of their approach in the domain of compact wearable devices by implementing simple and inexpensive hardware with very competitive false acceptance and false rejection rates (FAR and FRR), similar to fingerprint recognition, with only 1.02 heartbeats. Singh extracted a number of features including heartbeat intervals, inter-beat intervals and signal morphology based on fiducial points and then used Fisher's linear discriminant (FLD) analysis to select features for classification [40]. These selected features were compared to the registered ECG waveforms using the nearest neighbor criterion. In this case, it is a useful way to maximize the ratio of inter-subject scatter over intra-subject scatter, but the performance of rejection ratio for someone who was not registered in the database needs further investigation.

Uwaechia et al. presented a comprehensive review of biometric modalities based on ECG signals as a novel approach for human authentication [26]. They compared and analyzed the feature extraction methods (fiducial and non-fiducial feature extraction methods) and found that fiducial methods performed well on small databases and the non-fiducial methods are useful for a high performance ECG based biometric recognition system. They also observed that DNN approaches have better performance than conventional methods based ECG based biometrics.

Alduwaile et al. investigated the performance of various segmentation methods for ECG signals used in biometrics [41]. It was found that single-heartbeat segmentation based on R-peak provided the most accurate results among the fixed length, variable length, blind, and feature-dependent segmentation techniques. The blind method had lower accuracy and required a longer segmentation method to improve its results. Based on this, they used continuous wavelet transformation (CWT) to improve accuracy through entropy enhancement of short segmented signals [10]. In other words, in this case, fiducial point information such as R-peak is still required for segmentation, but for feature extraction, a non-fiducial feature extraction method is used to extract new features through domain transformation without using information such as fiducial points. The images converted to 2D time-frequency domain through CWT showed excellent performance with only short signals segmented for 0.5 seconds around the R-peak using CNN model. However, in terms of reliability, further research is needed to consider the fluctuation of signals under various cardiac conditions.

III. METHODOLOGY

Fig. 1 illustrates a schematic block diagram of the canine biometric system proposed in this paper. The system is composed of a dog ECG database and an integrated database, preprocessing for noise removal, segmentation to form input data for the biometric model, identification using DNNs, and finally performance verification and comparative analysis.

A. DATA SETS

In this work, two databases of canine ECG signals were used to distinguish the identity of dogs. One of these databases consisted of Holter monitoring data obtained during animal clinical research. However, since this database is not publicly accessible, we recognized that there may be constraints in verifying the objectivity of the results of this study, so we additionally conducted experiments using the PhysioZoo database [41], which is publicly accessible. Finally, we evaluated the biometric performance using an integrated dataset that combines two databases with different measurement equipment and environments. However, since the two datasets have different sampling rates, lead types, measurement resolutions, and measurement time lengths,

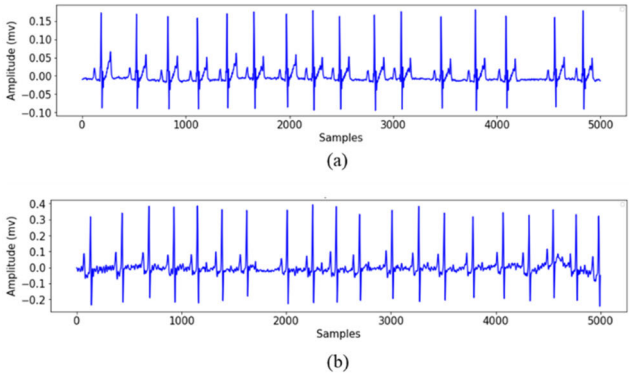

FIGURE 2. The example of ECG signals. (a) ECG signal from PhysioZoo. (b) ECG signals from Holter monitored data.

an additional unification process is required to integrate the two datasets into one dataset. The three databases were segmented through the R-peak-based window segmentation method and the blind segmentation method, respectively, for a total of six datasets. Fig. 2 shows an example of an ECG signal extracted from the two databases used in this study.

1) MAMMALIAN NSR (NORMAL SINUS RHYTHM) DATABASE FROM PHYSIOZOO

PhysioZoo is a collaborative and open platform for researching heart rate variability (HRV) in humans and mammals [42]. As part of their data release, PysioZoo has provided ECG measurement data for three types of mammals (dogs, rabbits, and mice) [43]. In this paper, the ECG data of the dog were used for biometric purposes. The database consists of one-channel ECG records from 17 subjects with a sampling frequency of 500 Hz. The surface electrodes for measurement were attached to both sides of the dog's chest with surgical tape, and all signals were measured while the dogs were awake and unmedicated prior to measurement.

The dog's ECG signals were recorded as normal sinus rhythm (NSR) in units of mV, but the dog's sex, breed, or age is not known. The length of the signal varied between subjects, ranging from a minimum of 4 minutes and 9 seconds to a maximum of 6 minutes and 48 seconds, with an average measurement time of 5 minutes and 31 seconds. The number of heartbeats per subject that can be identified by the number of R-peaks varies from a minimum of 330 to a maximum of 798. The ECG signals used in this experiment consist of a total of 5,610 heartbeats.

The data used in the experiment was based on the subject with the least number of heartbeats to maintain the same number of heartbeat waves per subject. Specifically, 330 ECG signals were randomly selected for R-peak based window segmentation. The resulting data was divided into an 8:2 ratio for training and testing and was followed by a 3-fold cross-validation. For the purpose of blind segmentation, 220 seconds of ECG signals were randomly selected per subject. The data was then divided into a ratio of 8:2 for training and testing, and was followed by a 3-fold cross-validation.

2) ECG DATABASE FROM HOLTER MONITORING

This database contains ECG signals from 16 subjects measured by Holter. Each signal was measured in microvolt units, and the subjects' gender and health status are unspecified. The dataset was solely obtained for clinical research purposes, not for animal biometric purposes by a private company, and is not publicly available. The signals were obtained using a 3-channel Holter monitor featuring 5 electrodes while the subjects were mobile, with a sampling rate of 512 Hz. The duration of the measured signal and the quantity of measurements differ among subjects. Specifically, the measurement time per file varies from a minimum of 40 seconds to a maximum of 21 hours and 25 minutes, but a minimum of 47 minutes was measured for each subject.

Each subject has a maximum of 167,837 heartbeat waves and a minimum of 3,300 heartbeat waves, and the dataset used in the experiment was based on the subject with the least number of heartbeats to maintain the same number of heartbeat waves per subject as in the case of the PhysioZoo database. For R-peak based window segmentation, 3,300 heartbeat waves were randomly chosen from channel 1 of the ECG signal for each subject. A total of 52,800 heartbeats utilized in the experiment were split 8:2 to create the data for training and testing, and a 3-fold cross-validation was conducted. With regards to blind segmentation, 1940 seconds of ECG signals were randomly chosen per subject, and the data was divided 8:2 for training and testing, and a 3-fold cross-validation was performed.

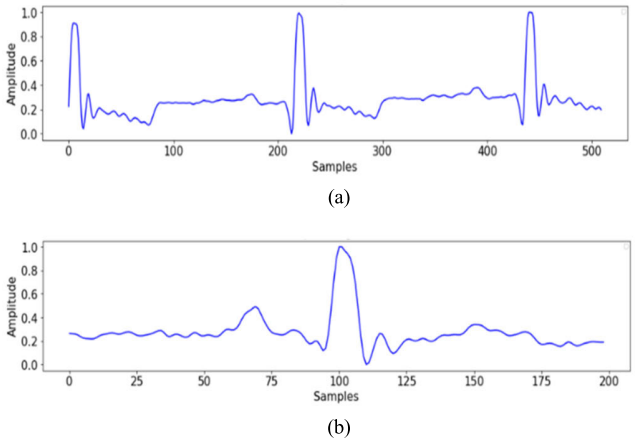

FIGURE 3. The example of segmented ECG signal. (a) R-peak based segmented signal. (b) Blind segmented signal.

3) INTEGRATED DATABASE

As previously mentioned, the above two databases were integrated to form a dataset for performance verification in order to evaluate biometric performance in a state where data from different measurement equipment and environments are mixed. The two datasets have different sampling rates, lead

types, resolutions, and lengths, so it is not possible to use the original data as it is, but the sampling frequency and amplitude units can be unified by the same standard. In other words, the units of millivolts and microvolts are unified, and the sampling frequency of Holter monitoring data is down sampled to 500 Hz to match the PhysioZoo data.

The integrated database consists of ECG records from a total of 33 subjects, and the size of the dataset used in the experiment was based on the subject with the lowest number of heartbeat waves to maintain the same amount of data per subject as in the case of the PhysioZoo database. For R-peak based window segmentation, 330 heartbeat ECG signals per subject were randomly selected and the data were split 8:2 for training and test, followed by 3-fold cross validation. For blind segmentation, 220 seconds of ECG signals per subject were randomly selected and the data were divided by 8:2 for training and test, then 3-fold cross validation was performed. Fig. 3 shows an example of a segmented ECG signal.

B. PREPROCESSING AND SEGMENTATION

Preprocessing and segmentation are required for each of the three sets of ECG raw signals to be utilized as input for the dog biometrics model. The initial step involves noise removal through preprocessing, followed by R peak detection to locate single heartbeats. Finally, the signals were segmented according to the window size based on the acquired R peak point and used as input for the model. In addition, a blind segmentation method was also experimented to compare the performance of the identification system.

TABLE 1. Normal ECG signals for dogs [20].

Parameters	values	units
Heart rate	Adult: 70-160	bpm
	Puppy: 70-200	
P wave amplitude	<0.4	mV
PR interval	60-130	ms
QRS amplitude	>0.5 and <3	mV
QT duration	150-250	ms

1) DENOISING AND NORMALIZATION

As shown in Table 1, the normal heart rate for dogs generally ranges from 70 to 160 beats/min, depending on the size of the dog. In puppies, a normal range is also considered to include rates up to 200 bpm [44]. The size of the R wave can range from 2.5 mV to 3 mV, depending on the size of the dog [45]. Dog ECG measurements have similar types of noise to human ECG measurements. However, animals often have more noise in their measurements than humans because it is difficult to ensure measurement uniformity in their environment.

Noise that can occur during ECG measurement includes muscle noise, electrical interface noise, baseline drift, and white noise. Muscle noise, also known as Electromyographic (EMG) noise, takes the form of irregular spikes with amplitudes typically ranging from 50 μV to 30 mV. It is caused by muscle movement and is relatively large in comparison to the ECG signal, often extending up to 10 kHz [38]. Muscle movements can occur not only during animal movements, but also during breathing or static conditions. Electrical interface noise can include 60 Hz noise from power lines and channel noise. Baseline drift or baseline wander noise is slow and low frequency noise that can be caused by poor skin-electrode contact, respiration, or body movement.

The ECG signals used in this paper are signals from which noise has been primarily removed in the hardware filter unit included in the measurement equipment. Consequently, baseline drift was generally insignificant and did not contain 60 Hz power line noise. Nonetheless, to eliminate any residual unconventional noise, a fourth-order Butterworth bandpass filter with a cutoff frequency of 0.5 Hz and 50 Hz was employed, taking into account the normal ECG frequency range. After removing abnormal amplitude noises, the signal's magnitude was normalized using the min-max normalization method.

2) R PEAK DETECTION AND WINDOW SEGMENTATION

For typical clinical analysis of ECG signals, fiducial points such as onset, offset and peak points of P wave, QRS complex and T wave are detected and used to obtain values including magnitude and interval of each wave. The measured ECG signals were segmented into a single heartbeat ECG signal and used as input. For this, the waveforms including P wave, QRS complex, T wave and U wave were segmented to be included in one window based on R peak location.

In this work, the stationary wavelet transform (SWT) algorithm was used to detect the R-peak. The wavelet transform (WT) has the advantage of bio-signal processing because it allows time-frequency representation and is widely used in ECG signal processing [29], [46]. Discrete wavelet transform (DWT) means to bisect the wavelet used in the continuous wavelet transform and scale it by discrete steps. The DWT can be generally described by the following equation [47].

$$\varphi_{j,k}(t) = \frac{1}{\sqrt{2^j}}\varphi\left(\frac{t - k2^j}{2^j}\right) \tag{1}$$

In (1), φ, j, and k represent the mother wavelet, the scale parameter, and the shift parameter, respectively. Based on this, the continuous wavelet transform (CWT) wavelet coefficient γ for the input signal $x(t)$ is defined as follows.

$$\gamma_{jk} = \int_{-\infty}^{\infty} x(t)\frac{1}{\sqrt{2^j}}\varphi\left(\frac{t - k2^j}{2^j}\right)dt \tag{2}$$

DWTs suffer from resolution loss due to down-sampling during the continuous wavelet transform. SWT can compensate

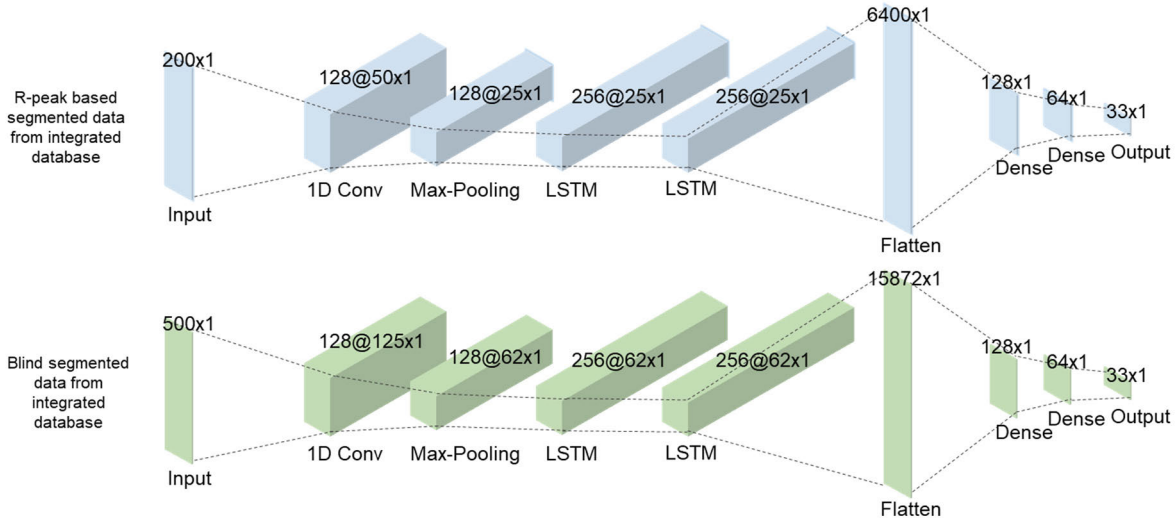

FIGURE 4. The architecture of the proposed DNN model for dog identification.

for this problem of DWT and is known to be more effective in denoising than DWT [48]. SWTs can be used to remove unwanted noise in the signals, followed by QRS complex detection and additional algorithms to find the R peak. The SWT is typically represented by the coefficients $c_{j,k}$ as follows.

$$c_{j,k} = \sum_{t \in z} x(t) \frac{1}{\sqrt{2^j}} \varphi \left(\frac{t - k2^j}{2^j} \right) \tag{3}$$

The R-peaks were detected using the Daubechies 3 (db3) wavelet function followed by applying a 3-level SWT [49]. Although the measured ECG signals were denoised using a bandpass filter, some spike-shaped noise remained, and these were sometimes mistakenly detected as R-peaks. To address this, we calculated the average amplitude of detected R-peak candidates and removed any peak points with values below 80% of the average value, which were considered noise and not R-peaks. The 80% threshold was determined heuristically through prior experience. Subsequently, 200 discrete data samples, each lasting approximately 400 ms, were divided into a window centered on the determined R-peak. Given that the PR interval varies inversely with heart rate within the range of 60-130 ms, a 400 ms length is deemed optimal for encompassing a singular heartbeat ECG signal [44].

3) BLIND SEGMENTATION

To compare the performance of different segmentation methods, in this study, in addition to segmenting the ECG signal into individual heartbeats based on R-peak, we also performed a blind segmentation method. In this case, blind segmentation entails dividing the ECG data into specific time intervals without any prior knowledge of the signals' fiducial points.

Research has been conducted on canine diseases and health conditions, specifically the relationship between atrial rate and QT interval [50], [51]. Nonetheless, applying research on fiducial points in human ECG signals directly to dogs is not feasible. This is owed to the significant variation in the range of QT and TT values in canine ECGs, and the challenge in generalizing the algorithm for finding fiducial points due to sinus arrhythmia leading to variation in heart rate compared to humans [18]. Therefore, in this study, we employed the blind segmentation method as well as the R-peak based window segmentation method. Blind segmentation does not require an algorithm to find the fiducial point, so it is relatively less computationally expensive than the R-peak based window segmentation method and is useful for fast processing. Nevertheless, there is no assurance that each segmented waveform includes a single R peak point or an entire single heartbeat ECG waveform. In this paper, the denoised ECG data was segmented at a rate of approximately 1 second (512 data samples). The data was segmented in such a way that it does not overlap with each other, so that no data is used redundantly. Table 2 indicates that adult dogs have a heart rate of 70-160 bpm while puppies have a heart rate of 70-200 bpm. This finding suggests that the most data blindly segmented at 1 second will have at least one complete heartbeat wave.

C. IDENTIFICATION MODEL

After preprocessing for noise reduction and segmentation of the canine ECG signal, the 1D_CNN-LSTM neural network shown in Fig. 4 was used to create the canine biometric model. The network consists of a deep learning architecture composed of one input layer, seven hidden layers, and one output layer. The network input dimensions are 200 × 1, 512 × 1, and 500 × 1, corresponding to R-peak based window segmentation, blind segmentation for Holter monitoring data, and blind segmentation for the integrated database, respectively. CNN is a deep learning method that effectively processes images and time-series data. It extracts features

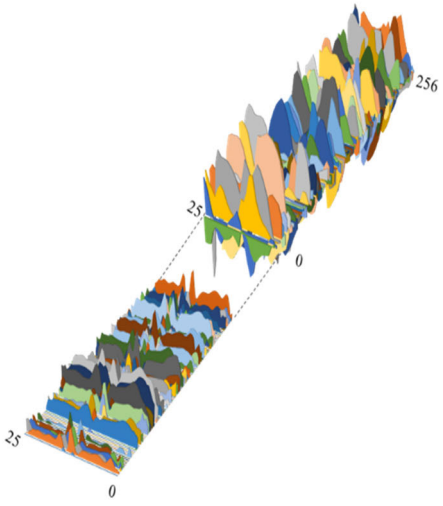

FIGURE 5. Example of 1D_CNN-LSTM intermediate output.

from input data using convolutional operations. The calculation of convolutional layers involves multiplying and adding input data with a moving kernel filter, as shown in (4).

$$Y(t) = X(t) * W(t) = \int_{-\infty}^{\infty} X(\tau) W(t-\tau) d\tau \quad (4)$$

In this equation, $X(t)$, $W(t)$, and $Y(t)$ represent the inputs, the kernel filter, and the feature map generated from the convolution operation. For optimal performance, we selected a kernel filter size of 33 after conducting numerous experiments. Additionally, to reduce the input data size by 1/4, a stride of 4 and zero padding were implemented before passing it to the next layer. In many related CNN-based studies for ECG signal processing, 2D CNNs have been trained with ECG image data as input. There have been other studies that utilize 1D CNNs to make use of ECG time-series features. In this study, we proposed a 1D CNN structure linked to an LSTM that does not require additional image transformations and can retain time-series features.

The detailed structure of the network is as follows. First, a 1D CNN was constructed to extract features and generate a feature map while maintaining the format of the ECG time-series data. Then, max-pooling was performed to reduce the dimensionality of the generated feature map by half. Fig. 5 is a part of the three-dimensional schematic of the 1D_CNN and feature map using 200 inputs constructed through R-peak based segmentation. That is the process of convolving 33 values equal to the kernel filter size in 4 strides among 200 single heartbeat input data samples composed of R-peak based segmented. Subsequently, the intermediate output passed through the 1D_CNN layer is expressed in the form of 128 line graphs in the form of 25 data flows. Based on the reduced dimensionality of the feature map, two layers of LSTM were added to extract sequential information of ECG signals. This allows the LSTM layers to learn sequential features from the time-series feature maps extracted and reduced by 1D CNN and max pooling.

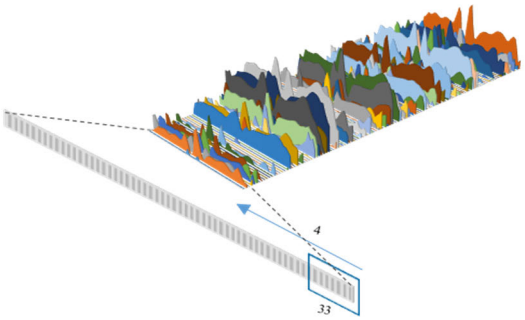

FIGURE 6. Example output from a 1D CNN.

Fig. 6 shows the intermediate output of the LSTM with the features obtained by 1D_CNN in Fig. 5 as input, represented by 256 line graphs consisting of 25 data streams. The outputs of the LSTM were flattened to convert the data into a one-dimensional vector and passed to the inputs of a subsequent dense layer. After passing through two additional dense layers, the final biometric results were obtained from the output layer, which consisted of 33 neurons. To produce the probability of each input value's predicted dog identification result, the softmax function was used in the output layer. After completion of the 1D convolution, a batch normalization was performed, and a dropout was applied to all layers except the input and output layers at the rate of 0.3. For LSTM layers, the cost was calculated in the last step, and the intermediate output of each step is fed to the next layer. The weights of all layers were initialized by the he initialization method.

IV. EXPERIMENT RESULTS

In this work, we conducted experiments in six scenarios depending on the dataset and segmentation method used to validate the dog identification performance. Specifically, Table 2 shows the details of the six datasets consisted of the following six datasets: the physioZoo dataset with R- peak based window segmentation, the physioZoo dataset with blind segmentation, the Holter dataset with

TABLE 2. Datasets scheme.

Dataset	Segmentation method	Length of segmented input data (samples)	Sampling frequency (z)	Number of Subjects	Number of inputs
Database from PhysioZoo	R-peak	200	500	17	5,610
	Blind	500	500	17	3,740
Database from Holter monitoring	R-peak	200	512	16	52,800
	Blind	512	512	16	31,040
Integrated database	R-peak	200	500	33	10,890
	Blind	500	500	33	7,260

R peak-based window segmentation, the Holter dataset with blind segmentation, the integrated dataset with R-peak based segmentation, and the integrated dataset with blind segmentation. The learning process was conducted for 150 epochs with a batch size of 32 and a learning rate of 0.0001. The Adam optimizer was used to adjust the parameters to minimize the loss function. For the performance evaluation, we compared the accuracy, equal error rate (EER) and the receiver operating characteristic curve (ROC) based on the confusion matrix of performance evaluation shown in Table 3.

TABLE 3. Confusion matrix scheme.

	Predicted Positive	Predicted Negative
Actual Positive	TP (True Positive)	FN (False Negative)
Actual Negative	FP (False Positive)	TN (True Negative)

A. RESULTS OF THE CANINE BIOMETRICS WITH THE SINGLE DATABASE

In order to compare and analyze the recognition performance of the DNN classifier with the 1DCNN_LSTM structure proposed in this study, three types of DNN classifiers (2D_CNN, 1D_CNN, and LSTM), which are commonly used as classifiers, were additionally constructed. The 2D_CNN classifier, which receives the ECG waveform as an image, consists of a 5-layer convolution layer with a kernel size of 3×3 and a 2-layer dense layer. The 1D_CNN classifier consists of 1 convolution layer and 2 dense layers with a kernel size of 33 and stride 4. LSTM classifier consists of two LSTM layers and two dense layers.

TABLE 4. Results of the identification accuracy.

Dataset	Segmentation method	Accuracy (%) 2D CNN	1D CNN	LSTM	Proposed model
PhysioZoo	R-peak	97.7	97.9	96.4	97.0
Holter	R-peak	97.2	98.5	98.5	98.7
Integrated	R-peak	95.4	96.9	94.9	96.3
PhysioZoo	Blind	82.6	51.1	72.8	94.9
Holter	Blind	93.2	87.1	92.1	96.9
Integrated	Blind	82.8	51.6	63.3	93.1

Table 4 shows the identification accuracy of the proposed recognition model and three additional DNN models for performance comparison in six experimental scenarios. The accuracy was calculated using (5) based on Table 3.

$$Accuarcy = \frac{TP + TN}{TP + FN + FP + TN} \tag{5}$$

As shown in Table 4, the R-peak based segmentation method showed high accuracy in both datasets, PhysioZoo database and Holter monitoring database, regardless of the type of classifier. When the PhysioZoo database was tested using R-peak based segmentation, the 2D_CNN method showed the highest accuracy, and the accuracy difference with the proposed method was 0.7%. When the Holter monitoring database was tested using R-peak based segmentation, the proposed method showed the highest accuracy of 98.7%, but in this case, the accuracy difference with the rest of the classifiers is not significant, ranging from a minimum of 0.2% to a maximum of 1.5%.

However, when blind segmentation was used, the performance difference between the classifier models was bigger, and the accuracy value was generally lower than that of the model with R-peak based segmentation. In particular, the accuracy of each model was significantly different in the test using the PhysioZoo database. This may be due to the fact that the amount of data in the PhysioZoo database is about one tenth less than that in the Holter monitoring database, so there was not enough training data. In the case of blind segmentation, a larger amount of training data is generally required because it does not have a process to extract only the required waveforms from the signals. In other words, the waveforms that are not extracted in a consistent form would increase the variability, and it is believed that learning is not performed properly with limited data. When the blind segmentation method was used, the proposed model showed the highest identification accuracy of 94.9% and 96.9% for the PhysioZoo database and the Holter monitoring database, respectively. The comparison models showed a minimum of 12.3% and a maximum of 43.8% difference in accuracy compared to the proposed method. When 1D_CNN was used for the PhysioZoo database, the accuracy was only 51.1%, which is very low compared to other classifiers. This is probably due to the fact that 1D_CNN could not properly learn the features of ECG signals, which have the characteristics of time series signals. In the case of 2D_CNN, there is a similar limitation in learning the features of the time-series signal, but it contains more information in one more dimension than 1D, so it may have been relatively useful to extract features in the convolution operation. In the test on the Holter monitoring database, the 1D_CNN model showed the lowest accuracy, but in this case the difference in accuracy was up to 9.8%. Also, when evaluated based on the average value of accuracy, the proposed model showed the highest identification rate with an average identification rate of 96.9%.

Fig. 7 visualizes the identification performance of the proposed method in the form of a confusion matrix. As shown in (a) of Fig. 7, the R-peak based segmentation on the PhysioZoo database showed no more than three recognition errors for each subject, except for 10 cases where subject 14 was misidentified as subject 7. Furthermore, the model never misidentified subject 7 as subject 14. In (c) of Fig. 7, the same database was tested with the blind segmentation method. In this case, there was no particular trend error in the recognition results of the remaining subjects, but the recognition error between subject 7 and subject 14 was relatively high. However, unlike (a) in Fig. 7, this time the highest recognition error was 7 times when subject 7 was misidentified as subject 14. In other words, while there were some cases where subject 14 was misidentified as subject 7 using R-peak based

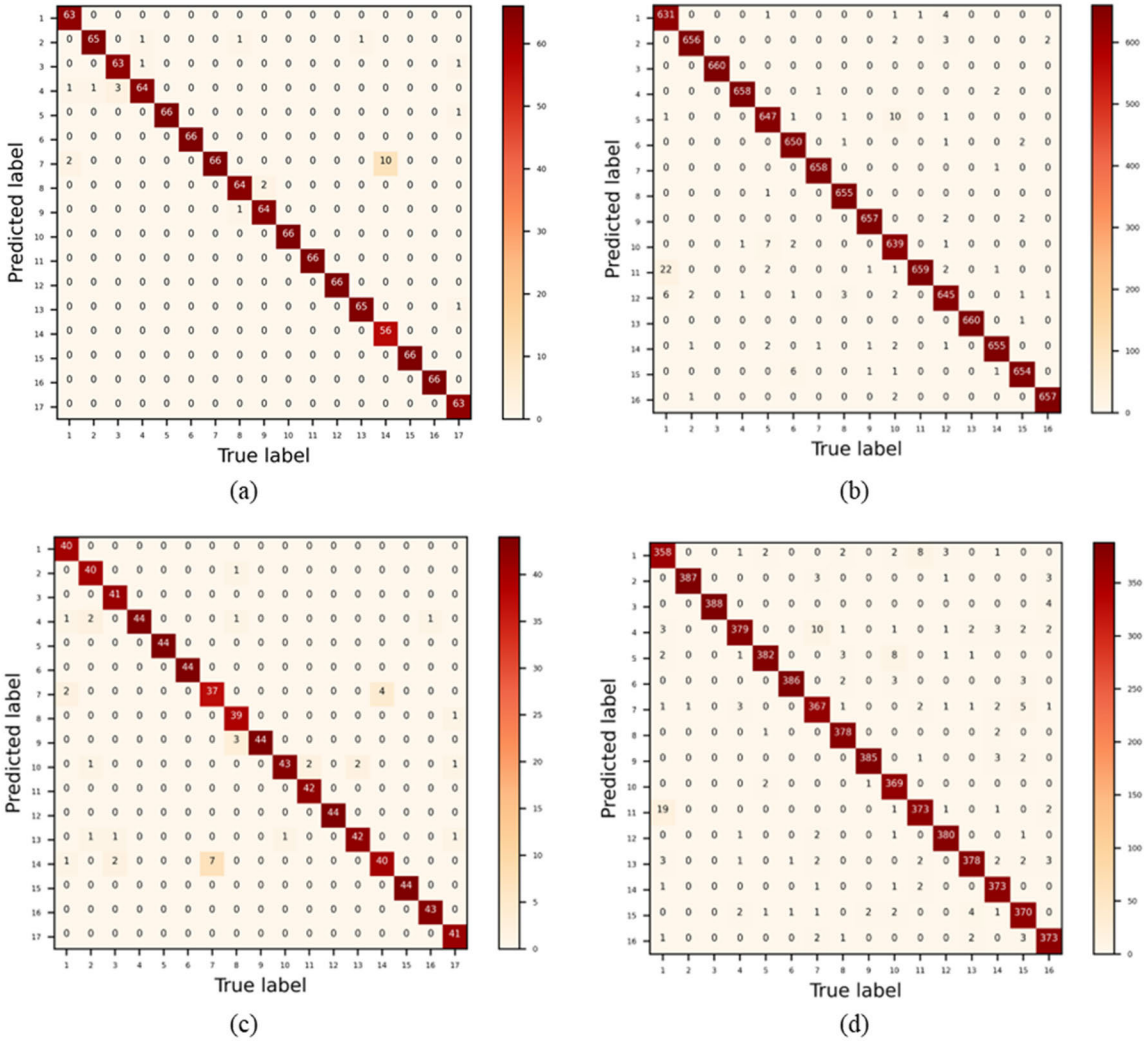

FIGURE 7. Confusion matrix of proposed model for single database. (a) result of R-peak based segmentation on the PhysioZoo database. (b) result of R-peak based segmentation on the Holter monitoring database. (c) result of blind segmentation on the PhysioZoo database. (d) result of blind segmentation on the Holter monitoring database.

segmentation, the recognition model could not clearly distinguish the difference between subject 7 and subject 14 using the blind segmentation method. When the Holter monitoring database was tested with the R-peak based segmentation method, the overall recognition rate increased, but the trend of the overall recognition rate was similar to the recognition results using the PhysioZoo database. In this case, the error of recognizing the subject 1 as the subject 11 was relatively larger in the identification using the Holter monitoring database. In the case of Fig. 7(b) and Fig. 7(d), the number of times subject 11 was misidentified as subject 1 was 4 and 8, respectively. In the case of Fig. 7(b), the error value of a particular subject was not significant. However, in Fig. 7(d), which is the recognition result using the blind segmentation method, there seems to be a problem in distinguishing between the two subjects (subject 1 and subject 11) as shown in Fig. 7(c). In the case of the proposed model, there is a variation in accuracy of about 2% depending on the segmentation method, and the difference seems to be due to the fact that the blind segmentation has a relatively large recognition error in distinguishing these two subjects.

B. RESULTS OF THE CANINE BIOMETRICS WITH INTEGRATED DATABASE

We evaluated the performance of the proposed model using an integrated database consisting of 33 subjects created by resampling data from the PhysioZoo database and the Holter monitoring database, and compared it with other models. As shown in Table 4, the accuracy of each identification model was as high as 94.9% when the R-peak based segmentation method was used. Also, the variation of accuracy by model was not significant as in the recognition performance results of individual databases. The best recognition rate was obtained by the 1D_CNN method with an accuracy of 96.9%,

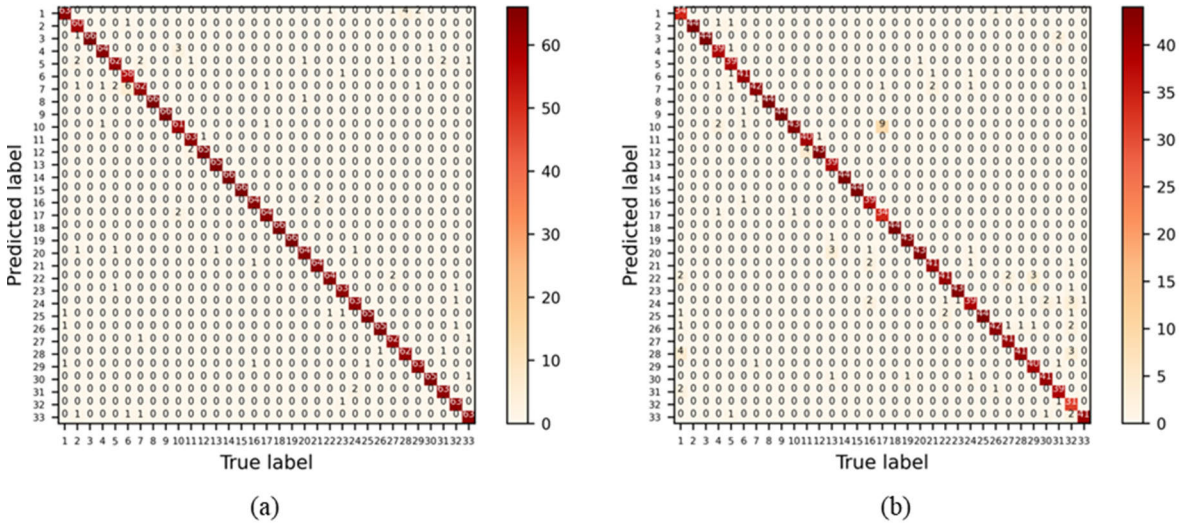

FIGURE 8. Confusion matrix of proposed model on the integrated databases. (a) result of R-peak based segmentation. (b) result of blind segmentation.

and the proposed model showed a close accuracy to 1D_CNN with 96.3%.

On the other hand, when the blind segmentation method was used for the identification test for the integrated database, the accuracy of each model was significantly different from before. In this case, the overall accuracy tended to be lower than when the R-peak based segmentation method was used, but the proposed model showed the highest accuracy of 93.1%, which was not significantly different from the identification performance for individual databases. The 1D_CNN showed the lowest accuracy for biometric recognition in the integrated database, and the LSTM model also showed only 63.3% accuracy. It is estimated that the reason for the decrease in recognition accuracy is due to the reduction in the number of data per subject while configuring the integrated database. In other words, when the 1D ECG signal is clearly segmented into the separate heartbeats and used as input, the 1D structure classifier can achieve sufficiently high accuracy recognition results, but in the blind segmentation method, the simple structure classifier has performance limitations.

Fig. 8 shows a visualization of the biometric results based on the proposed method in the form of a confusion matrix for integrated database. There is no particular trend in the misidentification results in Fig. 8(a) using the R-peak based segmentation method. In Fig. 8(b), the recognition rate of the subject 1 is relatively low. In this case, it is not a result of incorrectly identifying the subject 1 as a specific subject since the prediction results are not centered on a specific subject. In other words, there is no particular trend in the confusion matrix in both Fig. 8(a) and Fig. 8(b).

Table 5 shows the performance of the models in terms of equal error rate (EER). EER is a popular measure of biometric performance and can be obtained by (6), which is the error rate at the moment when the false acceptance rate (FAR) and the false rejection rate (FRR) match.

TABLE 5. Results of the model EER.

Dataset	Segmentation method	Accuracy (%) 2D CNN	1D CNN	LSTM	Proposed model
PhysioZoo	R-peak	0.63	2.20	1.05	0.74
Holter	R-peak	0.89	0.42	0.53	0.33
Integrated	R-peak	1.13	1.22	1.41	0.85
PhysioZoo	Blind	3.61	14.08	6.85	1.62
Holter	Blind	1.23	4.21	2.97	0.93
Integrated	Blind	4.04	11.41	9.19	2.09

$$EER = \frac{(FAR + FRR)}{2} \tag{6}$$

$$FAR = \frac{FP}{FP + TN} \tag{7}$$

$$FRR = \frac{FN}{TP + FN} \tag{8}$$

The overall trend of the EER values of each model was similar to the trend of the accuracy values of each model. In other words, the EER of the blind segmentation method was larger than that of the R-peak segmentation method, and the 1D_CNN model in particular showed a large performance variation depending on the segmentation method. When the R-peak based segmented PhysioZoo dataset was tested using the proposed identification model in this paper, the EER value was 0.14% higher than the 2D_CNN model, which showed the best EER value, but the proposed model showed the best EER value in the remaining biometric tests.

The receiver operating characteristic (ROC) curve shown in Fig. 9 illustrates the true positive rate (TPR) versus the false positive rate (FPR). In Fig. 9(a), the use of the R-peak based segmentation technique shows minimal deviation in the curve, which reflects the accuracy result. When using the

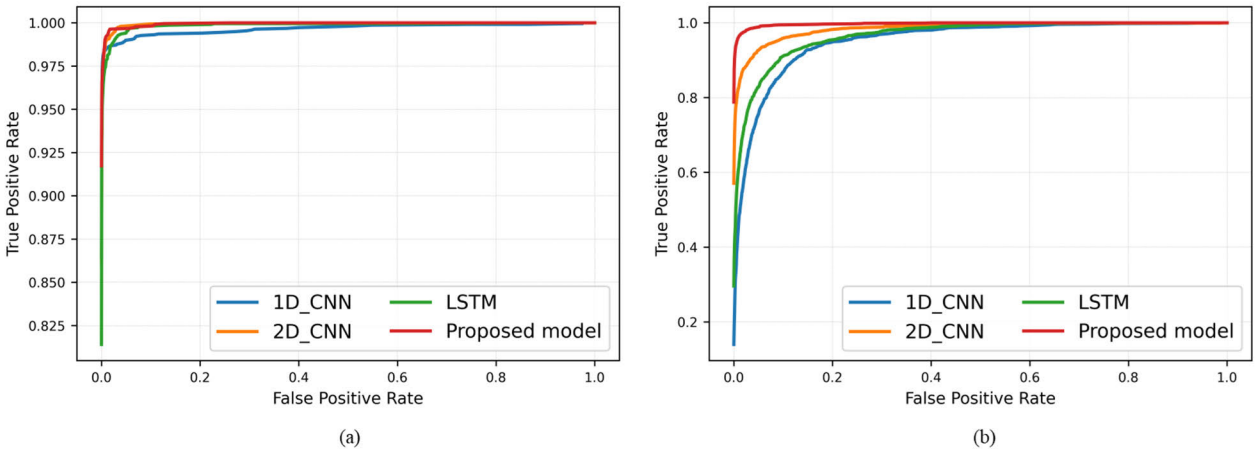

FIGURE 9. Comparison of ROC curves by classifiers. (a) ROC curves of integrated database with R-peak based segmentation. (b) ROC curves of integrated database with blind segmentation.

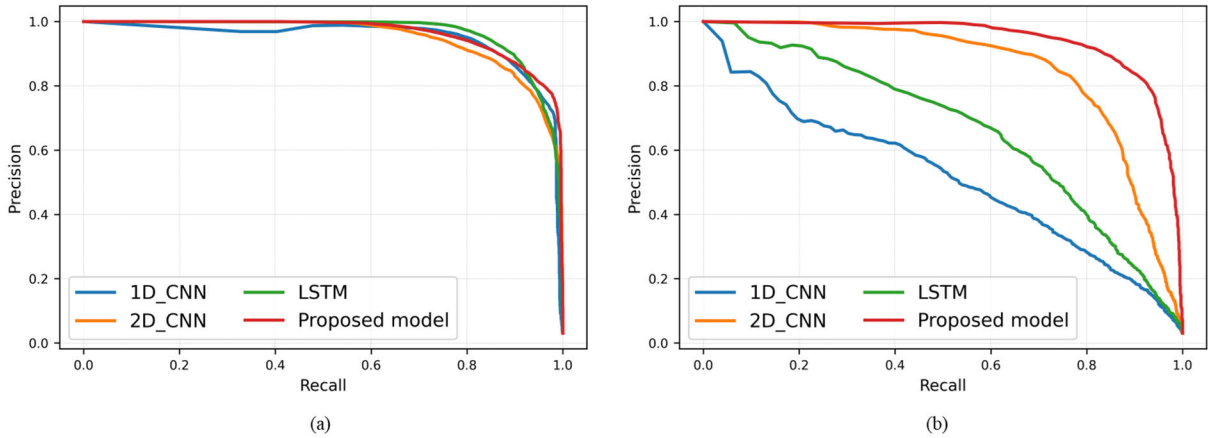

FIGURE 10. Comparison of PR curves by classifiers. (a) PR curves of integrated database with R-peak based segmentation. (b) PR curves of integrated database with blind segmentation.

blind segmentation method in Fig. 9(b), a variation in the curve by classifier was observed. As with the identification accuracy, the proposed model showed the highest performance with a ROC AUC (ROC area under the curve) value of 0.997. Note that for multiclass classification such as this problem, a distinct ROC curve should be displayed for each subject. However, here we plot the average of these results, which may make the models appear to perform better.

Fig. 10 shows the Precision-Recall (PR) curve of the model. The PR curve illustrates the performance of the model in a one versus rest (OvR) problem for multiclass classification. It can be compared to a data imbalance situation, and it has been reported that the PR curve is more useful than the ROC curve in this case to indicate the overall performance of the model. The results in Fig. 10 are similar to those in Fig. 9. For Fig. 10(a), there is no significant difference between the curves when using the R-peak based segmentation method, which is similar to Fig. 9(a). As for Fig. 10(b) using the blind segmentation method, the trend is similar to Fig. 9(b), but the difference between the values for each classifier is more obvious. The PR curve illustrates the performance of the proposed model, which means that the proposed model has excellent overall classification performance, not only specific values of TPR, FPR, precision and recall.

V. DISCUSSION

In this work, the preprocessed signals were used to construct a biometric data set using two methods, the R-peak based segmentation method and the blind segmentation method. In fact, two segmentation methods were applied to three databases, including the integrated database, and a total of six experimental datasets were constructed. The configured dataset was used for the biometric identification of dogs using the 1D_CNN-LSTM model proposed in this work. For the purpose of performance comparison with the proposed model, we constructed recognition models using 1D_CNN, 2D_CNN, and LSTM and performed biometric experiments on the same six datasets. First, we performed recognition experiments on two individual databases (PhysioZoo database, Holter monitoring database). By implementing

the R-peak based segmentation method, we demonstrated an accuracy of at least 96.4% in both databases. The variance in accuracy between the classifiers was only 1.5%. It was found that by using an appropriately segmented input signal of a single heartbeat wave through proper preprocessing, a high recognition rate can be achieved without much difference in accuracy among the types of DNNs used as classifiers. On the contrary, when blind segmentation was used, the recognition performance was generally worse than that of R-peak-based segmentation, and there was a significant difference in the recognition performance of each DNN model. Although the proposed model showed the best accuracy performance of 94.9% and 96.9% for the two databases, the recognition accuracy of the 1D_CNN model was 51.1%, which showed a significant decrease in the recognition rate compared to the R-peak based segmentation method. This problem can be attributed to the inability to recognize the temporal patterns in the ECG signal, as the input signal is segmented based on fixed time intervals, regardless of the position of the heartbeat waveform. The biometric test results of the integrated database, which merges two databases with different measurement environments and equipment, showed a similar trend to the biometric test results of the individual databases, in other words, when the R-peak based segmentation method was used, the recognition rates of the classifiers were all excellent without significant differences. However, when the blind segmentation method was used, the average recognition rate dropped to 72.7%. The decrease in recognition rate can be attributed to the lower accuracy of the blind segmentation method compared to the method that uses well-organized waveforms and additional signal processing as input. Insufficient input data may also have contributed to the problem. The blind segmentation method usually requires more training data. However, to evaluate the recognition performance including all subjects in the database, we set the criterion for the amount of data per subject based on the subject with the least number of single heartbeat waves, which may have caused the lack of training data. However, the proposed model in this research achieved a recognition accuracy of 93.1% even when the blind segmentation method was used, showing the least recognition degradation compared to the comparison model.

VI. CONCLUSION

In this paper, we proposed a method for dog identification based on canine ECG signals. The experiments used the Holter monitored ECG database of 16 dogs and the PhysioZoo database of 17 dogs. To investigate the biometric performance when signals from different measurement environments are included, we also performed biometric experiments on the biometrics of 33 dogs from the integrated database of these two databases. The raw ECG signals from the database were denoised using a bandpass filter and normalized. The proposed 1D_CNN-LSTM model in this study demonstrates at least 97.0% accuracy in recognizing dog biometrics based on individual databases utilizing R-peak segmentation, and at least 94.9% accuracy with the blind segmentation method. Results from integrating databases with varying measurement environments reveal recognition accuracy of 96.3% and 93.1% with R-peak and blind segmentation methods, respectively. In particular, the 1D_CNN-LSTM model proposed exhibits more than 10% increase in recognition accuracy compared to other models regarding biometrics with blind segmentation method under limited training data scenarios with discrepancy in the settings of data collection.

This study is significant because it represents the first attempt at canine ECG biometric recognition. The proposed model demonstrated superior recognition performance even when data from different measurement environments were combined. In addition, we developed a model structure with high biometric performance for simple input signals by using blind segmentation of 1D ECG signals instead of 2D image data. In situations where sufficient training data is available but complex recognition algorithms cannot be used, it may be more useful to use the recognition model proposed in this paper for a blind segmentation method that does not require additional processes such as distinguishing the individual heartbeat waves.

There is potential for further research related to this study. Additional data and follow-up experiments are needed to evaluate the performance of the proposed identification system. The database used in this paper contains data from multiple measurements of the same subject at different times, but does not contain information on the aging of the animal or changes in health status, so it is not possible to evaluate whether the proposed method can be used throughout the dog's lifetime. In addition, the appropriate input length of the model requires further validation. In our study, we analyzed 2-second datasets containing at least one individual heartbeat wave for blind segmentation. Further research is needed to evaluate and optimize the performance for different input lengths. Successful completion of such work could make the dog ECG biometric identification method applicable in many fields, including veterinary clinics and stray animal care services. In addition, the method using blind segmentation will be more easily applicable to biometric identification of animals other than dogs.

ACKNOWLEDGMENT

The authors would like to thank Hoyun Ltd. for allowing the use of their non-public data for this work and Han, Jeong Jae of Texas A&M University for providing the motivation for this research.

REFERENCES

[1] S. Gendelman, S. Biton, R. Derman, E. Zvuloni, J. Levy, S. Lugassy, A. Alexandrovich, and J. A. Behar, "PhysioZoo ECG: Digital electrocardiography biomarkers to assess cardiac conduction," *Proc. Comput. Cardiol. (CinC)*, Brno, Czech Republic, 2021, pp. 1–4, doi: 10.23919/CinC53138.2021.9662857.

[2] Health for Animals. (Sep. 2022). *How Many Pets are There in the World*. Global Trends in the Pet Population. [Online]. Available: https://www.healthforanimals.org/reports/pet-care-report/global-trends-in-the-pet-population/

[3] Best Friends. *The State of Animal Welfare Today*. [Online]. Available: https://network.bestfriends.org/sites/default/files/2023-06/National%20Shelter%20Data%20Set%202023_updated_6.12.2023.pdf

[4] *Lost and Found Animal Analysis for 2022*, document 12, Korean Animal Welfare Association, Mar. 2022. [Online]. Available: https://www.animals.or.kr/report/print/63402

[5] A. M. Johnston and D. S. Edwards, "Welfare implications of identification of cattle by ear tags," *Veterinary Rec.*, vol. 138, no. 25, pp. 612–614, Jun. 1996, doi: 10.1136/vr.138.25.612.

[6] S. Kumar, S. K. Singh, R. S. Singh, A. K. Singh, and S. Tiwari, "Real-time recognition of cattle using animal biometrics," *J. Real-Time Image Process.*, vol. 13, no. 3, pp. 505–526, Sep. 2017, doi: 10.1007/s11554-016-0645-4.

[7] S. Kumar and S. K. Singh, "Monitoring of pet animal in smart cities using animal biometrics," *Future Gener. Comput. Syst.*, vol. 83, pp. 553–563, Jun. 2018, doi: 10.1016/j.future.2016.12.006.

[8] H. B. Bae, D. Pak, and S. Lee, "Dog nose-print identification using deep neural networks," *IEEE Access*, vol. 9, pp. 49141–49153, 2021, doi: 10.1109/ACCESS.2021.3068517.

[9] K. W. Bowyer, K. Hollingsworth, and P. J. Flynn, "Image understanding for iris biometrics: A survey," *Comput. Vis. Image Understand.*, vol. 110, no. 2, pp. 281–307, May 2008, doi: 10.1016/j.cviu.2007.08.005.

[10] W. Yang, S. Wang, J. Hu, G. Zheng, and C. Valli, "A fingerprint and finger-vein based cancelable multi-biometric system," *Pattern Recognit.*, vol. 78, pp. 242–251, Jun. 2018, doi: 10.1016/j.patcog.2018.01.026.

[11] N. Narang and T. Bourlai, "Face recognition in the SWIR band when using single sensor multi-wavelength imaging systems," *Image Vis. Comput.*, vol. 33, pp. 26–43, Jan. 2015, doi: 10.1016/j.imavis.2014.10.005.

[12] R. Donida Labati, E. Muñoz, V. Piuri, R. Sassi, and F. Scotti, "Deep-ECG: Convolutional neural networks for ECG biometric recognition," *Pattern Recognit. Lett.*, vol. 126, pp. 78–85, Sep. 2019, doi: 10.1016/j.patrec.2018.03.028.

[13] D. A. AlDuwaile and M. S. Islam, "Using convolutional neural network and a single heartbeat for ECG biometric recognition," *Entropy*, vol. 23, no. 6, p. 733, Jun. 2021, doi: 10.3390/e23060733.

[14] S. Kumar, A. Pandey, K. S. R. Satwik, S. Kumar, S. K. Singh, A. K. Singh, and A. Mohan, "Deep learning framework for recognition of cattle using muzzle point image pattern," *Measurement*, vol. 116, pp. 1–17, Feb. 2018, doi: 10.1016/j.measurement.2017.10.064.

[15] S. Cho, J. Paeng, T. Kim, C. Kim, J. S. Kim, H. Kim, and J. Kwon, "Dog noseprint identification algorithm," in *Proc. Int. Conf. Inf. Netw. (ICOIN)*, Jeju Island, South Korea, Jan. 2021, pp. 798–800, doi: 10.1109/ICOIN50884.2021.9333973.

[16] S. S. Abdeldayem and T. Bourlai, "A novel approach for ECG-based human identification using spectral correlation and deep learning," *IEEE Trans. Biometrics, Behav., Identity Sci.*, vol. 2, no. 1, pp. 1–14, Jan. 2020, doi: 10.1109/TBIOM.2019.2947434.

[17] C. Min, H. D. Kim, and T. S. Kim, "ECG based user identification method using RBF neural networks," in *Proc. IEEK Conf.*, 2004, pp. 2531–2533.

[18] S. Kaese, G. Frommeyer, S. Verheule, G. van Loon, J. Gehrmann, G. Breithardt, and L. Eckardt, "The ECG in cardiovascular-relevant animal models of electrophysiology," *Herzschrittmachertherapie Elektrophysiologie*, vol. 24, no. 2, pp. 84–91, Jun. 2013, doi: 10.1007/s00399-013-0260-z.

[19] M. R. Gralinski, "The dog's role in the preclinical assessment of QT interval prolongation," *Toxicologic Pathol.*, vol. 31, pp. 11–16, Jan. 2003, doi: 10.1080/01926230390174887.

[20] H. S. Kühl and T. Burghardt, "Animal biometrics: Quantifying and detecting phenotypic appearance," *Trends Ecology Evol.*, vol. 28, no. 7, pp. 432–441, Jul. 2013, doi: 10.1016/j.tree.2013.02.013.

[21] B. Valarmathi, N. S. Gupta, G. Prakash, R. H. Reddy, S. Saravanan, and P. Shanmugasundaram, "Hybrid deep learning algorithms for dog breed identification—A comparative analysis," *IEEE Access*, vol. 11, pp. 77228–77239, 2023, doi: 10.1109/ACCESS.2023.3297440.

[22] A. Khosla, N. Jayadevaprakash, B. Yao, and L. Fei-Fei, "Novel dataset for fine-grained image categorization," presented at the First Workshop Fine-Grained Vis. Categorization (FGVC), IEEE Conf. Comput. Vis. Pattern Recognit. (CVPR), Colorado Springs, CO, USA, Jun. 2011.

[23] K. Lai, X. Tu, and S. Yanushkevich, "Dog identification using soft biometrics and neural networks," in *Proc. Int. Joint Conf. Neural Netw. (IJCNN)*, Budapest, Hungary, Jul. 2019, pp. 1–8, doi: 10.1109/IJCNN.2019.8851971.

[24] J. Liu, A. Kanazawa, D. Jacobs, and P. Belhumeur, "Dog breed classification using part localization," in *Proc. Euro. Conf. Comput. Vis. (ECCV)*, Florence, Italy, Oct. 2012, pp. 172–185.

[25] F. Shen, Z. Wang, Z. Wang, X. Fu, J. Chen, X. Du, and J. Tang, "A competitive method for dog nose-print re-identification," 2022, *arXiv:2205.15934*

[26] A. N. Uwaechia and D. A. Ramli, "A comprehensive survey on ECG signals as new biometric modality for human authentication: Recent advances and future challenges," *IEEE Access*, vol. 9, pp. 97760–97802, 2021, doi: 10.1109/ACCESS.2021.3095248.

[27] M. Merone, P. Soda, M. Sansone, and C. Sansone, "ECG databases for biometric systems: A systematic review," *Expert Syst. Appl.*, vol. 67, pp. 189–202, Jan. 2017, doi: 10.1016/j.eswa.2016.09.030.

[28] H. N. Jo, S. W. Park, H. G. Choi, S. H. Han, and T. S. Kim, "Development of an electrooculogram (EOG) and surface electromyogram (sEMG)-based human computer interface (HCI) using a bone conduction headphone integrated bio-signal acquisition system," *Electronics*, vol. 11, no. 16, p. 2561, Aug. 2022, doi: 10.3390/electronics11162561.

[29] G. Petmezas, K. Haris, L. Stefanopoulos, V. Kilintzis, A. Tzavelis, J. A. Rogers, A. K. Katsaggelos, and N. Maglaveras, "Automated atrial fibrillation detection using a hybrid CNN-LSTM network on imbalanced ECG datasets," *Biomed. Signal Process. Control*, vol. 63, Jan. 2021, Art. no. 102194, doi: 10.1016/j.bspc.2020.102194.

[30] E. Vallès, V. Bazan, and F. E. Marchlinski, "ECG criteria to identify epicardial ventricular tachycardia in nonischemic cardiomyopathy," *Circulat., Arrhythmia Electrophysiol.*, vol. 3, no. 1, pp. 63–71, Feb. 2010, doi: 10.1161/CIRCEP.109.859942.

[31] K. P. Tripathi, "A comparative study of biometric technologies with reference to human interface," *Int. J. Comput. Appl.*, vol. 14, no. 5, pp. 10–15, Jan. 2011.

[32] M. S. Islam, H. Alhichri, Y. Bazi, N. Ammour, N. Alajlan, and R. M. Jomaa, "Heartprint: A dataset of multisession ECG signal with long interval captured from fingers for biometric recognition," *Data*, vol. 7, no. 10, p. 141, Oct. 2022, doi: 10.3390/data7100141.

[33] R. Srivastva, A. Singh, and Y. N. Singh, "PlexNet: A fast and robust ECG biometric system for human recognition," *Inf. Sci.*, vol. 558, pp. 208–228, May 2021, doi: 10.1016/j.ins.2021.01.001.

[34] Y. Chu, H. Shen, and K. Huang, "ECG authentication method based on parallel multi-scale one-dimensional residual network with center and margin loss," *IEEE Access*, vol. 7, pp. 51598–51607, 2019, doi: 10.1109/ACCESS.2019.2912519.

[35] J. Laitala, M. Jiang, E. Syrjälä, E. K. Naeini, A. Airola, A. M. Rahmani, N. D. Dutt, and P. Liljeberg, "Robust ECG R-peak detection using LSTM," in *Proc. ACM Symp. Appl. Comput.*, Brno, Czech Republic, Mar. 2020, pp. 1104–1111.

[36] E. J. da Silva Luz, G. J. P. Moreira, L. S. Oliveira, W. R. Schwartz, and D. Menotti, "Learning deep off-the-person heart biometrics representations," *IEEE Trans. Inf. Forensics Security*, vol. 13, no. 5, pp. 1258–1270, May 2018, doi: 10.1109/TIFS.2017.2784362.

[37] Q. Zhang, D. Zhou, and X. Zeng, "HeartID: A multiresolution convolutional neural network for ECG-based biometric human identification in smart health applications," *IEEE Access*, vol. 5, pp. 11805–11816, 2017, doi: 10.1109/ACCESS.2017.2707460.

[38] J.-A. Lee and K.-C. Kwak, "Personal identification using an ensemble approach of 1D-LSTM and 2D-CNN with electrocardiogram signals," *Appl. Sci.*, vol. 12, no. 5, p. 2692, Mar. 2022, doi: 10.3390/app12052692.

[39] J. S. Paiva, D. Dias, and J. P. S. Cunha, "Beat-ID: Towards a computationally low-cost single heartbeat biometric identity check system based on electrocardiogram wave morphology," *PLoS One*, vol. 12, no. 7, Jul. 2017, Art. no. e0180942, doi: 10.1371/journal.pone.0180942.

[40] Y. N. Singh, "Human recognition using Fisher's discriminant analysis of heartbeat interval features and ECG morphology," *Neurocomputing*, vol. 167, pp. 322–335, Nov. 2015, doi: 10.1016/j.neucom.2015.04.063.

[41] D. Alduwaile and M. S. Islam, "Single heartbeat ECG biometric recognition using convolutional neural network," in *Proc. Int. Conf. Adv. Sci. Eng. (ICOASE)*, Duhok, Iraq, Dec. 2020, pp. 145–150, doi: 10.1109/ICOASE51841.2020.9436592.

[42] A. L. Goldberger, L. A. N. Amaral, L. Glass, J. M. Hausdorff, P. C. Ivanov, R. G. Mark, J. E. Mietus, G. B. Moody, C.-K. Peng, and H. E. Stanley, "PhysioBank, PhysioToolkit, and PhysioNet: Components of a new research resource for complex physiologic signals," *Circulation*, vol. 101, no. 23, pp. e215–e220, Jun. 2000, doi: 10.1161/01.cir.101.23.e215.

[43] J. A. Behar, A. A. Rosenberg, I. Weiser-Bitoun, O. Shemla, A. Alexandrovich, E. Konyukhov, and Y. Yaniv, "A novel open access platform for heart rate variability analysis of mammalian electrocardiographic data," *Frontiers Physiol.*, vol. 9, pp. 1–14, 2018, doi: 10.3389/fphys.2018.01390.
[44] R. Willis, P. Oliveira, and A. Mavropoulou, *Guide to Canine and Feline Electrocardiography*, 1st ed. Hoboken, NJ, USA: Wiley, 2018, pp. 349–350.
[45] R. B. Ford and E. M. Mazzaferro, "Diagnostic and therapeutic procedures," in *Kirk and Bistner's Handbook of Veterinary Procedures and Emergency Treatment*. Elsevier, 2006, pp. 449–572. [Online]. Available: https://www.ncbi.nlm.nih.gov/pmc/articles/PMC7158358/, doi: 10.1016/B0-72-160138-3/50005-9.
[46] Fauzani. N. Jamaluddin, S. A. Ahmad, S. B. M. Noor, W. Z. W. Hassan, A. Yaacob, and Y. Adam, "Performance of DWT and SWT in muscle fatigue detection," in *Proc. IEEE student Symp. Biomed. Eng. Sci. (ISSBES)*, Shah Alam, Malaysia, Nov. 2015, pp. 50–53, doi: 10.1109/ISSBES.2015.7435892.
[47] M. Merah, T. A. Abdelmalik, and B. H. Larbi, "R-peaks detection based on stationary wavelet transform," *Comput. Methods Programs Biomed.*, vol. 121, no. 3, pp. 149–160, Oct. 2015, doi: 10.1016/j.cmpb.2015.06.003.
[48] A. Kumar, H. Tomar, V. K. Mehla, R. Komaragiri, and M. Kumar, "Stationary wavelet transform based ECG signal denoising method," *ISA Trans.*, vol. 114, pp. 251–262, Aug. 2021, doi: 10.1016/j.isatra.2020.12.029.
[49] M. Chafii, J. Palicot, and R. Gribonval, "Wavelet modulation: An alternative modulation with low energy consumption," *Comp. Rendus Phys.*, vol. 18, no. 2, pp. 156–167, Feb. 2017, doi: 10.1016/j.crhy.2016.11.010.
[50] A. S. Davis and B. J. Middleton, "Relationship between QT interval and heart rate in Alderley Park beagles," *Veterinary Rec.*, vol. 145, no. 9, pp. 248–250, Aug. 1999, doi: 10.1136/vr.145.9.248.
[51] S. G. Dennis, N. J. Summerfield, and A. Boswood, "Investigation of QT-interval dispersion in the electrocardiogram of 81 dogs," *Veterinary Rec.*, vol. 151, no. 3, pp. 77–82, Jul. 2002, doi: 10.1136/vr.151.3.77.

MIN KEUN CHO received the B.S. degree in information, communications, and electronics engineering from The Catholic University of Korea, Bucheon-si, South Korea, in 2017 and 2022, respectively. His main research interests include the machine learning and deep learning of battery, semiconductor defect inspection systems, and the development of health care systems.

TAE SEON KIM received the B.S. and M.S. degrees in electrical engineering from Inha University, Inchon, South Korea, in 1991 and 1993, respectively, and the Ph.D. degree from the School of Electrical and Computer Engineering, Georgia Institute of Technology, Atlanta, in 1998.

He was a Postdoctoral Research Fellow with the Packaging Research Center (PRC), Georgia Institute of Technology, in 1999, and a Senior Research Engineer with Samsung Electronics, from 1999 to 2001. He is currently a Professor with the School of Information, Communications, and Electronics Engineering, The Catholic University of Korea, Bucheon-si, South Korea. He is the author of more than 80 technical articles and more than 15 inventions. His research interests include the development of intelligent systems and their application to real systems, including healthcare systems and modeling, optimization, and the control of semiconductor manufacturing processes.